JOURNAL OF TRAFFIC AND TRANSPORTATION ENGINEERING (ENGLISH EDITION) 2022; 9 (2): 244–260

Available online at www.sciencedirect.com

ScienceDirect

journal homepage: www.keaipublishing.com/jtte

Original Research Paper

A semi-empirical model for top-down cracking depth evolution in thick asphalt pavements with open-graded friction courses

Francesco Canestrari, Lorenzo Paolo Ingrassia*, Amedeo Virgili

Dipartimento di Ingegneria Civile, Edile e Architettura (DICEA), Università Politecnica delle Marche, Ancona 60131, Italy

HIGHLIGHTS

- The semi-empirical model predicts TDC depth as a function of the traffic loads.
- The model is sigmoidal with a maximum TDC depth assumed equal to 150 mm.
- The model parameters depend on the properties and the age of the OGFC.
- In-situ observations provide a preliminary validation of the model.
- The model can be used in a PMS to identify pavement areas where TDC is critical.

ARTICLE INFO

Article history:
Received 3 February 2021
Received in revised form 3 June 2021
Accepted 22 June 2021
Available online 7 April 2022

Keywords:
Top-down cracking (TDC)
Asphalt pavement
Open-graded friction course (OGFC)
Porous asphalt (PA)
Pavement management system (PMS)
Modelling

ABSTRACT

Thick asphalt pavements with open-graded friction course (OGFC) are exposed to top-down cracking (TDC), a distress consisting of longitudinal cracks that initiate on the pavement surface close to the wheel path and propagate downwards. The main objective of this study is to develop a semi-empirical model for the prediction of TDC depth evolution for such pavements. For this purpose, a series of cores were taken from different Italian motorway pavements affected by TDC and analyzed in the laboratory. Cracked cores taken from the wheel path area were analyzed to determine TDC depth, whereas intact cores taken from the middle of the lane (not affected by traffic loadings) were tested to obtain the volumetric and mechanical properties of the OGFC mixture. The proposed model, developed on the basis of the results already available in literature and on the findings of the laboratory investigation, predicts the evolution of TDC depth as a function of the applied traffic loadings (in terms of 12-ton fatigue equivalent single axle loads, i.e., ESALs). The model is sigmoidal with a maximum TDC depth assumed equal to 150 mm. The shape parameter of the sigmoidal function depends on the indirect tensile strength (ITS) of the OGFC mixtures (which takes into account indirectly also the volumetrics and stiffness of the OGFC), whereas the evolutive translation factor depends on the age of the OGFC mixture. After excluding some outliers, the model was able to predict the measured TDC depth very well. Moreover, in-situ observations allowed a preliminary validation of the proposed model. This model can be used in pavement management systems (PMSs) to plan

* Corresponding author. Tel.: +39 071 220 4780; fax: +39 071 220 4780.
E-mail addresses: f.canestrari@univpm.it (F. Canestrari), l.p.ingrassia@pm.univpm.it (L.P. Ingrassia), a.virgili@univpm.it (A. Virgili).
Peer review under responsibility of Periodical Offices of Chang'an University.
https://doi.org/10.1016/j.jtte.2021.06.001

surface repairs due to TDC in a timely manner, thus minimizing pavement damage and maintenance costs.

1. Introduction

Many existing asphalt pavements have been designed based on the minimization of bottom-up cracking and rutting of the unbound layers, which have long been considered as the major distresses affecting the structural properties of the pavement (ARA Inc, 2004). This approach, still used in several countries, has led to the construction of increasingly thick and stiff pavements, in order to reduce the tensile stress/strain at the bottom of the asphalt layers (responsible for bottom-up cracking) and the compression stress/strain at the top of the unbound layers (responsible for rutting).

As a consequence, a different type of distress, named as top-down cracking (TDC), has begun to be observed more and more frequently on asphalt pavements in the last decades, as first reported by several authors between the 1980s and the 2000s (Baladi et al., 2003; Dauzats and Rampal, 1987; Gerritsen et al., 1987; Harmelink and Aschenbrener, 2003; Hugo and Kennedy, 1985; Matsuno and Nishizawa, 1992; Pellinen et al., 2004; Wambura et al., 1999). TDC consists of longitudinal cracks that initiate on the pavement surface close to the wheel path and then propagate downwards. The development of TDC is related to the local tire-pavement contact stresses, which determine the onset of tensile and shear stresses at or near the wheel path. Therefore, due to the localized nature of the phenomenon, increasing the pavement thickness (or stiffness) is not an effective solution to counteract TDC (Canestrari and Ingrassia, 2020; Luo et al., 2018).

Just like bottom-up cracking, TDC is ascribable to fatigue failure, which consists in the progressive degradation of the material properties due to the application of cyclic loads (smaller than the material strength). Therefore, TDC evolves affecting increasing portions of the asphalt layer thickness, gradually compromising the structural properties of the pavement. In fact, after the initiation, cracks evolve vertically until a certain depth, then they progressively deviate towards the center of the wheel path reaching angles of 20°–40° with respect to the vertical plane. Consequently, if parallel cracks generated close to the right and left edge of the tire connect one to each other, a generalized failure in the upper part of the asphalt layers may occur. The concurrent evolution of TDC on the pavement surface includes an initial phase in which a single longitudinal crack appears close to the wheel path, followed by the formation of parallel cracks 0.3–1.0 m distant (the so-called "sister cracks") and finally by the formation of short transverse cracks connecting the longitudinal ones, leading to an alligator cracking-like pattern concentrated within the wheel path (Canestrari and Ingrassia, 2020; Luo et al., 2018).

It has been demonstrated that, for thick asphalt pavements, TDC can be more critical than bottom-up cracking. Nikolaides and Manthos (2019) showed, through numerical simulations, that it is possible to define a thickness of the asphalt layers above which TDC is the predominant fatigue failure mechanism (instead of bottom-up cracking). Analogously, the analysis of thick pavements with the viscoelastic continuum damage (VECD) approach showed that for such pavements damage can be more concentrated on the pavement surface rather than at the bottom of the asphalt layers (Mun et al., 2004; Roque et al., 2010). These results are consistent with the findings by Uhlmeyer et al. (2000), who investigated the condition of existing pavements in the state of Washington and observed that the pavements affected by TDC had an average asphalt layer thickness of 160 mm, whereas the average asphalt layer thickness for the pavements affected by bottom-up cracking was equal to 110 mm. In summary, TDC can affect all pavements, but for thin pavements bottom-up cracking is predominant over TDC, whereas for thick pavements TDC precedes bottom-up cracking (Canestrari and Ingrassia, 2020).

TDC development strongly depends on the characteristics of the wearing layer, which is the first to counteract the distress. In this regard, TDC is particularly detrimental for pavements with open-graded friction courses (OGFCs), also known as porous asphalt (PA) pavements (Canestrari and Ingrassia, 2020). Nowadays, OGFCs are used worldwide (where the climatic conditions allow their use) as the wearing layer of highways and high speed roads, because they significantly improve the safety conditions at high speeds by reducing aquaplaning risks (that cause loss of tire-pavement skid resistance/friction) and splash & spray phenomena (that decrease the driver's visibility). The water drainage is ensured by the high air void content of the asphalt mixture, which is usually between 15% and 25%. However, the high air void content is also responsible for reduced mechanical properties (in terms of fracture strength) and lower durability (i.e., accelerated aging due to the greater exposure to oxygen, atmospheric agents and UV radiation) as compared to typical dense-graded mixtures. In addition, air voids represent flaws in the material from which micro-cracks can easily arise (Wu et al., 2020). Therefore, in the presence of OGFCs, pavements tend to fail because of TDC rather than bottom-up cracking, regardless of the other boundary conditions, as demonstrated by Nikolaides and Manthos (2019) with a numerical simulation. This was also confirmed by a recent survey carried out on Italian motorway pavements (Ingrassia et al., 2020), which are typically thick pavements formed by a wearing layer of 4 cm, a binder layer of 8 cm, a base layer of 15 cm and a cement-bitumen treated or cement-stabilized subbase of 25 cm. The survey involved a trial network of about 400 km belonging to four different Italian motorways with different characteristics in terms of geometry, traffic level, wearing layer type and climate. It was found that TDC can affect up to 30% of the slow traffic lane length for pavements with OGFC, whereas TDC was totally absent in the trial section with dense-graded wearing layer. Nevertheless, the TDC issue is often underestimated in the design and the maintenance of OGFCs, also due to the lack of knowledge of the phenomenon by practitioners. Moreover, only few scientific studies have addressed the TDC issue for open-graded mixtures so far (Chen et al., 2012; Koh, 2009).

Beside the traffic loadings, the pavement structure and the characteristics of the wearing layer mixture, there are also other factors affecting TDC development. The phenomenon is accelerated in the presence of strong stiffness gradients determined by aging and/or climatic conditions. Moreover, mixture segregation and poor compaction during the pavement construction promote the development of the distress, whereas thermal effects can cause TDC in the case of extreme climatic conditions (Canestrari and Ingrassia, 2020).

Several mechanistic (Ling et al., 2019; Roque et al., 2010) or statistical (Shen et al., 2016) TDC prediction models exist in literature. Even though they are based on a solid theoretical background, these models might be impractical for operational purposes (e.g., maintenance), especially for practitioners. In addition, most of the existing propagation models focus on the longitudinal growth of TDC distress rather than on its depth evolution. However, the prediction of TDC depth is more meaningful from the maintenance point of view, as the progressive worsening of the pavement structural properties is basically ascribable to the depth evolution of the cracks and therefore a critical TDC depth should be defined in the perspective of surface maintenance/repairs. Moreover, the definition of a longitudinal propagation model requires less efforts in terms of control cores to be taken from the pavement, but in this way other types of longitudinal cracks could be misidentified as TDC (thus affecting the model accuracy). In this regard, the recent survey carried out by Ingrassia et al. (2020) on Italian motorway pavements highlighted that surface cracks caused by heavy vehicles tire blowout and cracks due to longitudinal joints in the presence of entry/exit lanes, narrow emergency lanes or in the case of carriageway widening can be located in the wheel path area and thus wrongly identified as TDC. From the survey, it also emerged that surprisingly the concentration of cracks due to heavy vehicles tire blowout can be even higher than TDC.

Within this context, the main objective of this study is to develop a practical and reliable semi-empirical model for TDC depth evolution in thick pavements with OGFC, to be used for pavement maintenance. For this purpose, a series of cores were taken from Italian motorway pavements affected by TDC and analyzed in the laboratory. The results of the laboratory investigation (i.e., TDC depth, volumetric and mechanical properties of the OGFC) were used, together with the corresponding traffic data, to develop a sigmoidal model able to predict the evolution of TDC depth as a function of the applied traffic loadings, taking into account the effect of the age and the properties of the OGFC mixture. A flowchart of the activities carried out is shown in Fig. 1.

2. Laboratory investigation

2.1. *Coring campaign*

Thirteen sampling points, in which the pavement was affected by TDC, were selected along the Italian motorway trial network recently analyzed by Ingrassia et al. (2020). As

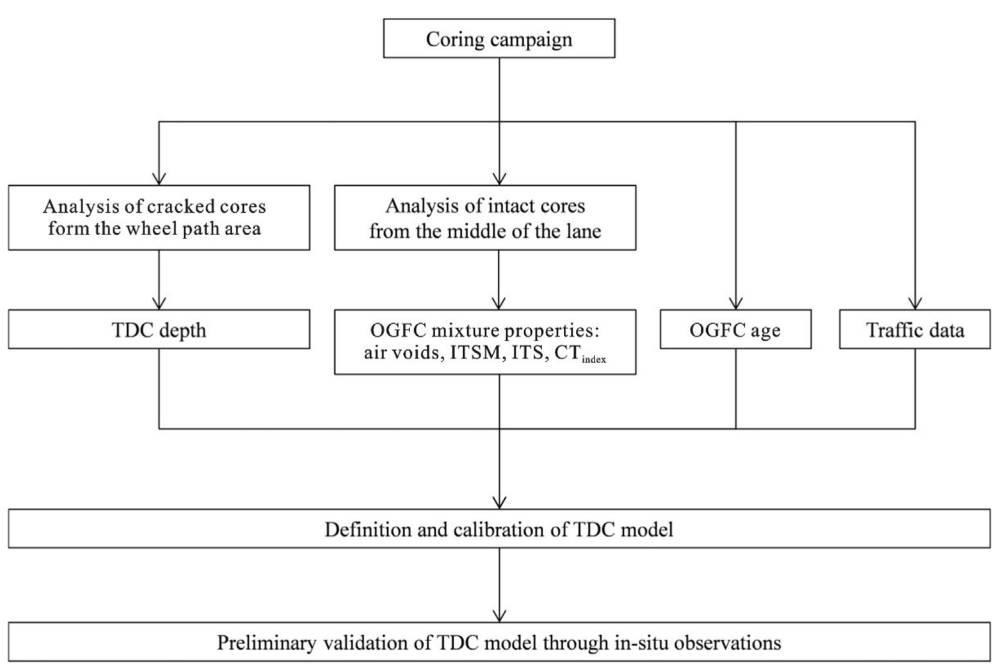

Fig. 1 – Flowchart of the activities carried out.

Table 1 – Sampling points on the motorway network.

Sampling point	Motorway	Carriageway	Mileage (km)	OGFC age (years)	12-ton ESALs	9-ton super-singles
1	A1	South	156 + 500	8	1.15E+08	4.94E+07
2	A14	South	67 + 600	10	8.70E+07	3.52E+07
3	A1	North	180 + 630	13	1.73E+08	7.43E+07
4	A1	North	157 + 780	5	7.72E+07	3.32E+07
5	A1	North	151 + 460	6	7.56E+07	3.29E+07
6	A1	North	131 + 120	6	7.76E+07	3.37E+07
7	A1	South	132 + 760	8	9.99E+07	4.34E+07
8	A1	South	165 + 790	13	1.70E+08	7.30E+07
9	A1	South	172 + 700	4	6.32E+07	2.72E+07
10	A1	South	173 + 760	4	6.32E+07	2.72E+07
11	A1	South	175 + 700	4	6.32E+07	2.72E+07
12	A1	South	177 + 220	13	1.73E+08	7.46E+07
13	A1	South	188 + 520	6	1.10E+08	4.72E+07

can be seen from Table 1, the sampling points selected are characterized by a different OGFC age (i.e., the period between the OGFC laying and the coring campaign) and a different number of traffic loadings applied during the OGFC in-service life.

As for the traffic loadings, the equivalent single axle loads (ESALs) were computed starting from the actual traffic data monitored over time, considering a 12-ton single axle with twin wheels as reference axle. For the determination of the load equivalency factors (LEFs), the approach first proposed by the Norwegian Road Research Laboratory (Evensen and Senstad, 1992) was considered. This approach allows to take into account the effects of axle type, tire type and tire inflation pressure, and differentiates the LEF value based on the distress to be examined. For the case of interest, since TDC is ascribable to fatigue failure, fatigue cracking was considered as the reference distress in the calculation of the LEFs. For each sampling point, Table 1 also reports the number of 9-ton super-singles, calculated with the same approach. In fact, the growing use of super-singles (also known as wide base tires) in commercial vehicles instead of dual tires is most likely one of the main causes of the relatively recent diffusion of TDC, as super-singles are responsible for greater damage to the pavement with respect to dual tires (COST 334, 2001; Foley and Sharp, 2001). Other factors that probably contributed to the appearance of TDC on asphalt pavements in the last decades are the progressive replacement of bias ply tires with radial tires and the related increase in the tire inflation pressure. In fact, radial tires cause higher contact stresses with the pavement as compared to bias ply tires, and the contact stresses are even higher in the case of wide base radial tires (Myers et al., 1999). All these aspects were properly taken into account through the approach adopted for the definition of the LEFs.

It is worth noting that for the coring operations it was necessary to narrow the motorway carriageway (i.e., reduction of the number of lanes available for the in-service traffic). Consequently, where possible, consecutive sampling points (less than 2 km away) were selected in order to operate a single narrowing, and only the right wheel path of the slow traffic lane was considered to limit the carriageway narrowing. Moreover, in order to facilitate the identification and coring operations (all carried out at night for safety reasons and to avoid possible queues), only sections where the distress was clearly visible were considered. In addition, to avoid the possible influence of inertial loading effects, only straight sections were taken into consideration. In summary, taking into account also the complexity of the coring operations, the data collected from the analysis of the cores should be acknowledged as extremely valuable. It is also worth mentioning that several other cores not listed in Table 1 were taken along the investigated motorway network, leading to "false" TDC, i.e., cracks mainly attributable to longitudinal joints and tire blowouts, as documented by Ingrassia et al. (2020).

For each sampling point, 2 full-depth cores were taken along the TDC crack in the wheel path, about 10–20 m apart from each other. In addition, 1 OGFC core was taken from the intact pavement area in the middle of the lane. Hereinafter, the cores taken in the wheel path and the cores taken in the middle of the lane are also referred to as "cracked cores" and "intact cores", respectively.

The laboratory investigation consisted in two main parts.

- The cracked cores were visually examined to determine TDC depth (Section 2.2).
- The intact cores were subjected to volumetric analyses and mechanical tests to determine the properties of the OGFC mixture (Section 2.3).

2.2. *Analysis of cracked cores*

The cracked cores taken from the wheel path area were visually examined to identify the longitudinal crack type and, in the case of TDC, to assess the crack depth.

Specifically, the whole core was examined at first, then each core was cut vertically perpendicular to the wheel path direction. In this way, it was possible to observe the internal section of the core (Fig. 2), not affected by the consequences of the coring operations. Afterwards, the total crack depth was measured for every core affected by TDC. Since two cracked

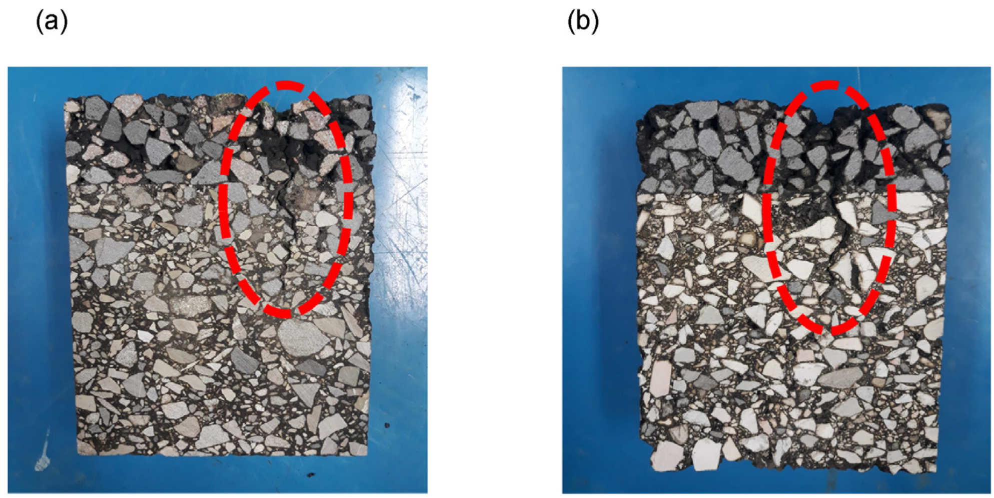

Fig. 2 – Internal section of cracked cores. (a) Example 1. (b) Example 2.

cores were taken for each sampling point, the average TDC depth was then calculated.

The values of the average TDC depth obtained are summarized in Table 2. It can be noted that TDC depth is between 11 mm (sampling point 3) and 190 mm (sampling point 12). In two cases (sampling points 4 and 5), the surface cracks observed on the pavement surface were at the early initiation stage. Nevertheless, it was decided to test the corresponding intact cores anyway in order to have more data available on the characteristics of the OGFC mixtures.

Together with the traffic data (Table 1) and the results obtained from the analysis of the intact cores (Section 2.3), these values were used to calibrate the proposed model (Section 3.3).

2.3. *Analysis of intact cores*

The volumetric properties of the OGFC at the sampling points were assessed by determining the air void content of the intact cores. To calculate the air void content of the specimens, some assumptions were necessary because of the slight composition differences between the cores. Specifically, the bulk density of the specimens (EN, 2020) was calculated by assuming in all cases a nominal binder content of 5% by aggregate weight (typical binder content for OGFC in Italy) and a bulk density of the aggregates of 2.701 g/cm^3 (based on the typical gradation curve of Italian OGFC mixtures).

The stiffness of the intact cores was evaluated by measuring the indirect tensile stiffness modulus (ITSM) with the Nottingham Asphalt Tester (NAT). The tests were carried out according to the Annex C of the standard EN (2018) at a temperature of 20 °C.

After the ITSM tests, the cores were subjected to ITS tests, performed according to the standard EN (2017) at a temperature of 25 °C and a deformation speed of 50 mm/min. This testing temperature is prescribed by the technical specifications of the Italian Highway Agency (Autostrade per l'Italia, 2018).

In addition to the ITS parameter, another synthetic index was determined from the analysis of the load-displacement curve obtained from the test. The expression of this index, known as CT_{index}, is the following.

$$CT_{index} = \frac{t}{62}\frac{G_f}{|m_{75}|}\frac{l_{75}}{D} \tag{1}$$

where t is the specimen thickness (mm), G_f is the fracture energy, $|m_{75}|$ and l_{75} are, respectively, the absolute value of the tangent slope and the displacement at the post-peak point at which the load is equal to 75% of the peak load, D is the specimen diameter. Specifically, G_f is obtained by dividing the fracture work W_f (i.e., the area under the load-displacement curve) by the cracking face area (given by the specimen diameter D multiplied by the specimen thickness t), whereas $|m_{75}|$ is obtained from the load and displacement values at the post-peak points at which the load is equal to 65% and 85% of the peak load.

The CT_{index} was introduced by the Texas A&M University research group to quantify the cracking resistance of asphalt mixtures within the framework of the so-called indirect tensile asphalt cracking test (IDEAL-CT) and has its theoretical foundation in fracture mechanics. Specifically, this index is based on the Paris law and on the work done by Bazant and

Table 2 – Average TDC depth measured on the cracked cores.

Sampling point	Average TDC depth (mm)
1	80.0
2	100.0
3	11.0
4	0.0
5	0.0
6	35.0
7	78.5
8	120.0
9	140.0
10	112.5
11	122.5
12	190.0
13	66.5

Prat about crack propagation in concrete (Im and Zhou, 2017; Zhou et al., 2017). Given its definition, higher CT_{index} values indicate better cracking performance of the asphalt mixture.

It is known that currently no laboratory test method is universally acknowledged as suitable to evaluate the TDC performance of asphalt mixtures. Most of the test methods proposed for TDC are typically used to investigate the performance in terms of bottom-up cracking or reflective cracking (Chen, 2020; Zhou et al., 2016), whereas few of the proposed methods are normally used to study the shear properties of the asphalt mixture (Ma et al., 2018; Sun et al., 2018). Other test methods have been expressly developed to characterize the TDC performance of asphalt mixtures (Chen et al., 2013; Roque et al., 2004), but they are less consolidated.

Among the numerous test methods/approaches proposed in literature (Canestrari and Ingrassia, 2020), the CT_{index} approach appears promising for several reasons. Firstly, the IDEAL-CT test is totally analogous to the ITS test, which is very simple, fast and already used as a routine test in many countries, and the CT_{index} can be easily obtained from the analysis of the load-displacement curve, even though its definition is based on fracture mechanics theory. Moreover, the IDEAL-CT test is suitable for the characterization of wearing layer cores taken from the pavement, as the specimen thickness required is between 38 and 75 mm (Im and Zhou, 2017; Zhou et al., 2017) and the wearing layers typically have a thickness of 40–50 mm. In addition, previous studies suggested that the IDEAL-CT test is characterized by a good repeatability (as compared to other cracking tests), and the CT_{index} is well correlated with TDC field performance and sensitive to most of the asphalt mixture properties (e.g., aging, presence of reclaimed asphalt, binder type and content) (Chen, 2020; Im and Zhou, 2017; Zhou et al., 2017).

The volumetric and mechanical properties obtained from the analysis of the intact cores are summarized in Table 3. The cores taken at sampling points 5 and 6 were damaged during the coring operations and thus it was not possible to test them.

Table 3 – Volumetric and mechanical properties of the intact cores.

Sampling point	Air void content (%)	ITSM (MPa)	ITS (MPa)	CT_{index}
1	25.0	4427	0.69	8.3
2	28.4	4234	0.69	7.5
3	20.7	5099	0.88	15.7
4	13.9	4996	1.10	16.9
5	Specimen damaged during the coring operations			
6	Specimen damaged during the coring operations			
7	19.9	6393	1.00	5.4
8	25.3	4014	0.73	13.7
9	16.4	7550	0.99	6.3
10	15.9	6988	1.08	10.7
11	24.0	2801	0.54	15.7
12	20.1	6004	0.99	29.5
13	19.5	5493	0.71	5.3

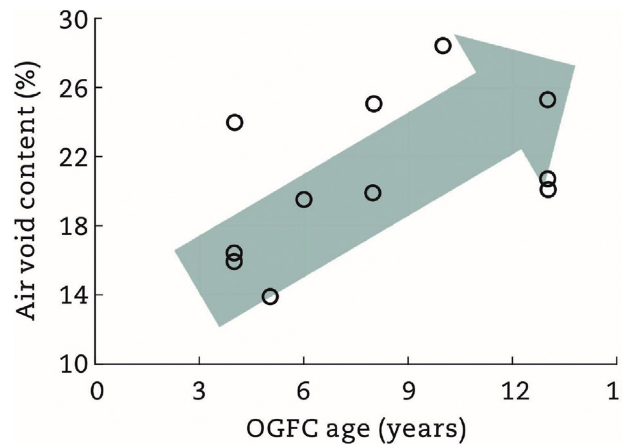

Fig. 3 – Air void content vs. OGFC age.

In Fig. 3, the air void content of the specimens is represented as a function of the OGFC age. It can be noted that the range of air void contents is wide, from a minimum of about 14% to a maximum of more than 28%. Moreover, Fig. 3 shows that more recent OGFCs are generally characterized by lower air void contents. This finding is consistent with the changes of the technical specifications adopted by the Italian Highway Agency in recent years, which have been oriented towards the use of OGFCs with air void contents lower than 18%–20%, whereas a target air void content of 20%–22% was typically prescribed in the past.

The relationships between air void content and ITS and between air void content and ITSM are shown respectively in Fig. 4(a) and (b). It can be observed that both mechanical parameters decrease as the air void content increases, as expected. A clear linear correlation exists between the volumetric and the mechanical properties of the tested cores, even though the values of the coefficient of correlation R^2 are not very high. The non-perfect correlation can be explained by considering that the cores were taken from different motorway sections, and therefore they were characterized by different ages and compositions. In addition, it should be pointed out that it was not possible to strictly comply with the test protocols in all cases due to the imperfect geometry of some cores (caused by the inevitable ravelling of the OGFC mixture during the coring operations). Nevertheless, the fitting correlations obtained would lead to values of ITS and ITSM respectively equal to about 1.5 MPa and 9000 MPa for dense-graded mixtures prepared with SBS-polymer modified bitumen compacted at 2.5% air void content, perfectly in line with the typical values determined experimentally for this type of asphalt concrete.

The reliability of the experimental data is confirmed also by the clear relationship between ITS and ITSM values, shown in Fig. 5. The pairs of ITS-ITSM values are aligned along a straight line passing through the origin with a coefficient of correlation R^2 close to 1.

Conversely, no meaningful information emerges from the results in Fig. 6(a) and (b), showing the CT_{index} as a function of air void content and ITS, respectively. The experimental data are scattered and inconclusive, even though higher CT_{index} should be expected for mixtures with a greater cracking

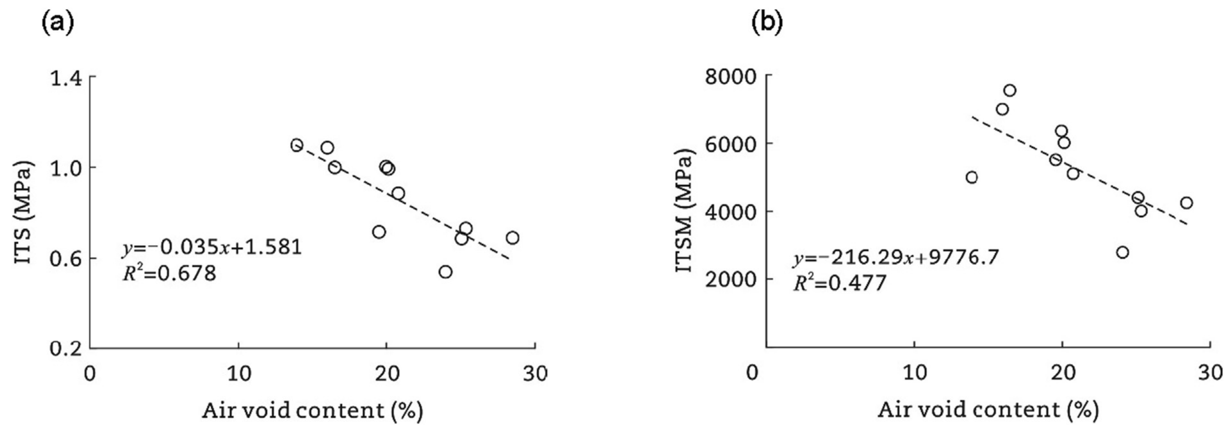

Fig. 4 – Effect of air void content. (a) ITS. (b) ITSM.

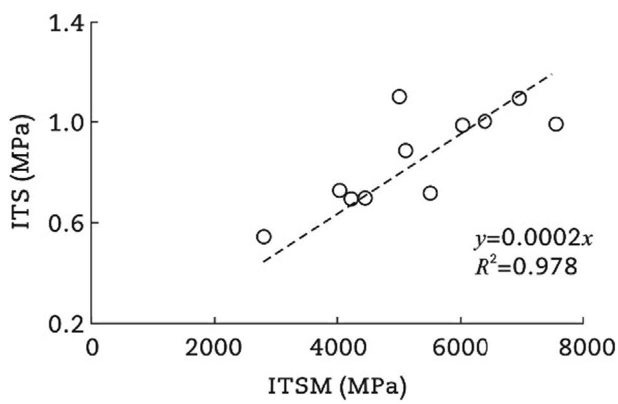

Fig. 5 – ITS vs. ITSM.

resistance (Eq. (1)). Instead, a certain trend between ITSM and CT_{index} can be observed from Fig. 7. Specifically, if we exclude one data that is clearly out of trend, it can be noted that the CT_{index} tends to decrease as the stiffness of the mixture increases, consistently with the fact that stiffer materials are characterized by a more brittle behavior and a lower fracture resistance.

3. TDC depth evolution model

In this section, an evolutive model is proposed for the prediction of TDC depth as a function of the traffic loadings and the main factors affecting the phenomenon. The model is developed based on the results available in literature, the outcomes of previous surveys on Italian motorway pavements (Ingrassia et al., 2020) and the findings of the laboratory investigation on extracted cores (Section 2).

The proposed model could be implemented in a pavement management system (PMS), with the aim of planning surface maintenance due to TDC in a timely manner, thus minimizing pavement damage and maintenance costs. In fact, given the high stiffness of Italian motorway pavements, TDC initiation occurs earlier than bottom-up cracking initiation, and therefore it is necessary to predict the frequency of surface maintenance before a full-depth rehabilitation is needed due to bottom-up cracking.

3.1. *Background and hypotheses*

As already explained in Section 1, the initiation and propagation of TDC are strongly determined by the repeated traffic loadings. Even though it is known that the phenomenon is closely related to the peculiar characteristics of heavy vehicles' super-singles (Section 2.1), from Table 1 it can be observed that the number of applied super-single loads is equal to the number of 12-ton fatigue ESALs, except for a conversion factor that is constant for a given traffic spectrum (equal to about 2.3 for motorway A1 and 2.5 for motorway A14). Therefore, the proposed model expresses TDC depth evolution as a function of 12-ton fatigue ESALs, as the latter are more used (especially in Italy).

In this sense, the model is similar to that proposed by Kumara et al. (2004), who suggested a third order polynomial relationship between ESALs and TDC depth. The significant difference with that model, however, lies in the definition of a parametric function that allows to take into account the main experimental evidence through a semi-empirical approach, giving due importance to the performance and the age of the wearing layer mixture. This aspect is one of the main original contributions provided by this study.

Among the volumetric and mechanical parameters taken into consideration in the analysis of the intact cores (Section 2.3), the parameter adopted to characterize the performance of the OGFC is the ITS. This choice is motivated by the simplicity and the diffusion of such routine test, along with the correlations observed between the ITS values and the air void content (Fig. 4(a)) as well as between the ITS values and the ITSM values (Fig. 5). In fact, in light of these correlations, it emerges that, for a fixed age (i.e., a fixed aging degree of the mixture), the ITS parameter is closely linked to the volumetric and stiffness characteristics of the open-graded mixture. On the other hand, the CT_{index} parameter did not show satisfactory correlations with the experimental data collected (Section 2.3), probably because the studies that propose such parameter are focused on dense-graded

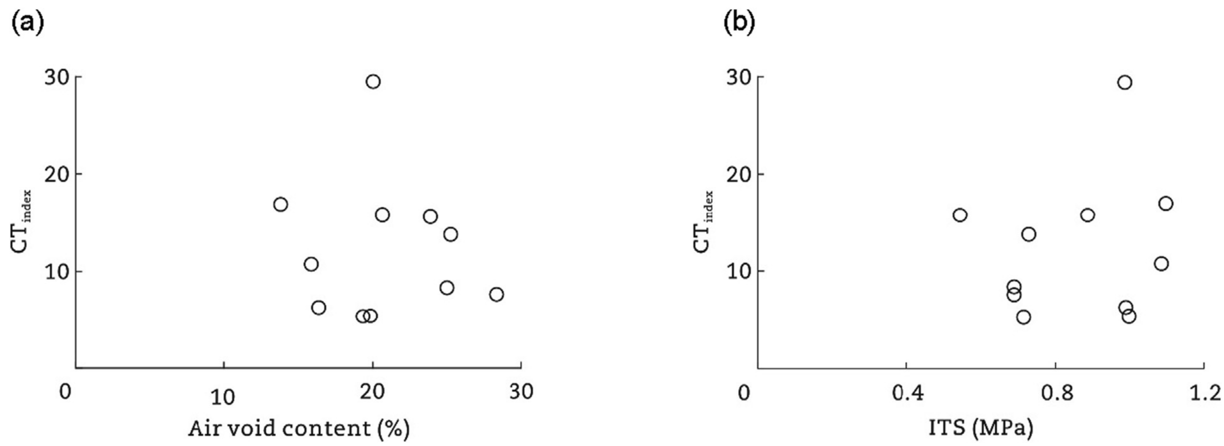

Fig. 6 – Effect on CT_{index}. (a) Air void content. (b) ITS.

mixtures, whereas this study focuses on open-graded mixtures. It is worth noting that the outcomes of this study may represent a milestone in the scientific literature, as for the first time an attempt is being made to examine the TDC phenomenon in a systematic way in the case of open-graded mixtures with polymer modified bitumen (SBS) (in most cases containing an amount of reclaimed asphalt pavement, RAP, up to 15%). Consequently, the results already available in literature may not be valid for the case of interest, because in most situations they refer to unmodified dense-graded mixtures.

Moreover, it should be pointed out that the calibration of the model was carried out considering only the characteristics of the OGFC, even though TDC affects also the binder layer in most of the examined cores (Section 2.2). Although such an hypothesis makes the model approximate, it can be considered acceptable from an engineering point of view for the following reasons. Firstly, as compared to the initiation phase, the propagation phase is less affected by the properties of the mixture due to the high stress level concentrated at the crack tip, according to the principles of fracture mechanics (basically, a dense-graded mixture tends to behave like an open-graded mixture in the presence of a crack). In addition, for Italian motorway pavements, the structural continuity between OGFC and binder layer is ensured by the use of a tack coat with a high dosage of polymer modified residual bitumen, as prescribed by the technical specifications. Finally, it should be underlined that the proposed model intends to provide a realistic estimate of TDC depth (not an exact prediction) at the most critical points of in-service pavements in the context of a PMS, with the aim of highlighting the necessity of deeper pavement monitoring and controls when the conditions (in terms of traffic, mixture properties and/or pavement age) are crucial.

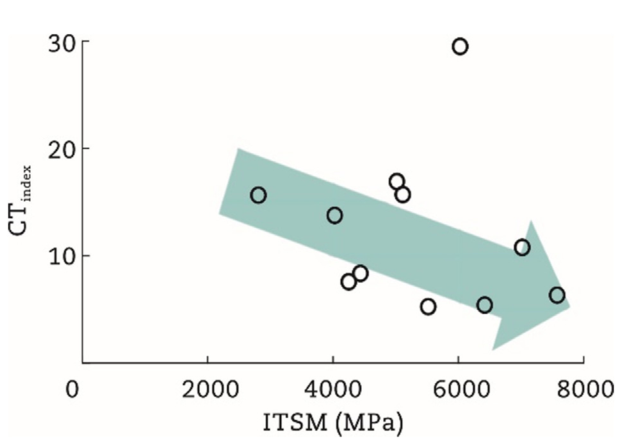

Fig. 7 – Effect of ITSM on CT_{index}.

Another important aspect taken into account in the proposed semi-empirical model is the definition of a maximum TDC depth. In fact, from the literature it is known that the crack initially propagates in the vertical direction, but after a certain depth it progressively tends to form angles up to 40° with respect to the vertical plane due to the overall stress state, which is determined not only by the local tire-pavement interactions but also by the global response of the pavement to the applied loads (Myers and Roque, 2002). This was corroborated by the visual examination of the cracked cores taken from the motorway network, as shown in Fig. 8(a) and (b). In general, TDC cracks started to deviate from the vertical direction at about 10 cm of depth, in the binder layer. The observation of the cracked cores also confirmed the existence of a maximum depth after which TDC tends to propagate in a sub-horizontal direction, as can be seen from Fig. 8(c). This final stage in the depth evolution of the distress corresponds to the final stage of TDC evolution on the pavement surface, i.e., a cracking pattern formed by parallel longitudinal cracks connected by short transverse cracks with a possible generalized failure in the upper part of the asphalt layers (as discussed in Section 1).

As for the value of the maximum TDC depth, field observations indicate that the depth of the cracks usually does not exceed half the thickness of the asphalt layers (Roque et al., 2010). For a typical Italian motorway pavement, the total thickness of the asphalt layers is about 30 cm. Therefore, it seems reasonable to assume a maximum TDC depth of 15 cm. Moreover, for Italian motorway pavements, such depth typically corresponds to the interface between the binder layer and the base layer, which generally represents a structural discontinuity in the pavement that may facilitate the sub-horizontal propagation of TDC.

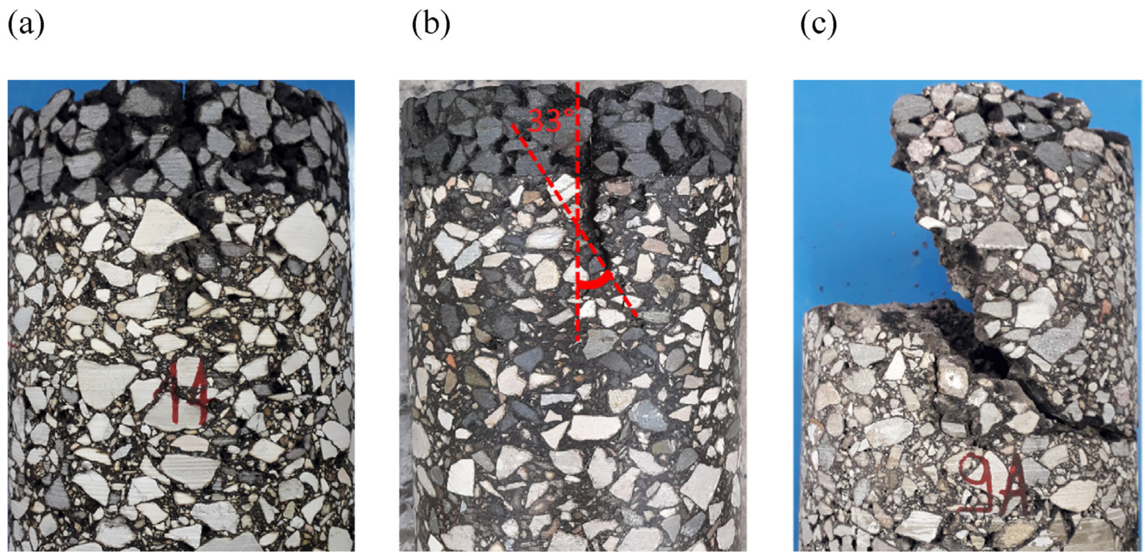

Fig. 8 – Evolution of top-down crack. (a) Initial stage. (b) Intermediate stage. (c) Final stage.

3.2. Description and analysis of the model

The semi-empirical model proposed to predict the evolution of TDC depth as a function of the number of 12-ton fatigue ESALs (N) is expressed by the following parametric equation.

$$TDC(N) = TDC_{max} e^{-\left(\frac{A}{N}\right)^B} \tag{2}$$

where TDC_{max} is the maximum TDC depth (assumed equal to 15 cm, as explained in Section 3.1), A and B are model parameters that depend on the characteristics of the OGFC mixture.

Eq. (2) can be rewritten in a normalized form in order to obtain a sigmoid $P(N)$ whose values are between 0 and 1.

$$P(N) = \frac{TDC(N)}{TDC_{max}} = e^{-\left(\frac{A}{N}\right)^B} \tag{3}$$

It is worth noting that the proposed function is sigmoidal, just like the law introduced by other authors (Ling et al., 2019; Lytton et al., 2018) to describe the longitudinal growth of TDC on the pavement as a function of time. Even the American Mechanistic-Empirical Pavement Design Guide (MEPDG) considers a sigmoidal transfer function between fatigue damage and TDC longitudinal growth (ARA Inc, 2004). The evolution of the distress in the longitudinal direction is highly correlated with the depth evolution, and therefore it is reasonable to assume a similar law (sigmoidal) for the two phenomena.

To analyze the meaning of the parameter B, let us consider two values of the number of 12-ton fatigue ESALs (N_1 and N_2) and calculate the corresponding values of the sigmoid (P_1 and P_2).

$$P_1 = P(N_1) = e^{-\left(\frac{A}{N_1}\right)^B} \quad \text{and} \quad P_2 = P(N_2) = e^{-\left(\frac{A}{N_2}\right)^B} \tag{4}$$

By applying the logarithm to the natural base to both sides of the equations, we obtain

$$\ln(P_1) = -\left(\frac{A}{N_1}\right)^B \quad \text{and} \quad \ln(P_2) = -\left(\frac{A}{N_2}\right)^B \tag{5}$$

By dividing Eq. (5) member by member, we arrive at

$$\frac{\ln(P_1)}{\ln(P_2)} = \left(\frac{N_2}{N_1}\right)^B \quad \text{or} \quad \ln\left[\frac{\ln(P_1)}{\ln(P_2)}\right] = B \ln\left(\frac{N_2}{N_1}\right) \tag{6}$$

Therefore, the parameter B can be obtained as follows.

$$B = \frac{\ln\left[\frac{\ln(P_1)}{\ln(P_2)}\right]}{\ln\left(\frac{N_2}{N_1}\right)} \tag{7}$$

From Eq. (7), it can be deduced that B determines the shape of the sigmoid, and thus it is a shape parameter.

To better clarify the meaning of the parameter A, let us consider now two sigmoids characterized by the same B parameter but different A parameters ($A_1 \neq A_2$). If we consider the same P^* value for both sigmoids, we have

$$P^* = e^{-\left(\frac{A_1}{N_1}\right)^B} = e^{-\left(\frac{A_2}{N_2}\right)^B} \tag{8}$$

The previous relationship is valid only if the following condition occurs.

$$\frac{A_1}{N_1} = \frac{A_2}{N_2} \quad \text{or} \quad \frac{N_2}{N_1} = \frac{A_2}{A_1} \tag{9}$$

By applying the logarithm (to the natural base or to the base 10, indifferently) to both members of the second equality in Eq. (9), we obtain

$$\ln(N_2) - \ln(N_1) = \ln\left(\frac{A_2}{A_1}\right) \quad \text{or} \quad \log(N_2) - \log(N_1) = \log\left(\frac{A_2}{A_1}\right) \tag{10}$$

In summary, Eq. (10) indicates that two sigmoids having the same shape parameter B are characterized by points that are translated (in a logarithmic scale) by an amount equal to the logarithm of the ratio between their A parameters. Therefore, A is a translation factor and the term N/A in Eq.

(3) represents the "normalized N", i.e., the normalized number of ESALs.

A graphical representation of the concepts introduced is provided in Figs. 9 and 10. The influence of the parameter B on the shape of the sigmoid can be observed from Fig. 9, where the value of A was set as $A = a \times 10^8$, with $a = 1.00$. The choice of introducing the parameter a, which is scaled by a factor equal to 10^8 with respect to A, is motivated by the necessity to simplify the fitting of the model to the experimental data (discussed in Section 3.3), a phase in which also the number of 12-ton fatigue ESALs (N) is scaled by the same factor.

Specifically, from the sigmoids shown in Fig. 9 related to values of B equal to 0.3, 0.5 and 0.7 with a set equal to 1.00, it can be observed that, as the shape parameter B increases, the sigmoid tends to a steeper trend determined by an anti-clockwise rotation around a point with abscissa $N = A$. For higher B values, such rotation implies a delay in the initiation of the crack (i.e., the initial horizontal branch of the sigmoid translates to the right) followed by a more rapid propagation phase and an earlier achievement of the final stage of the distress (due to the concurrent translation to the left of the final horizontal branch of the sigmoid).

The influence of the translation factor A on the sigmoid can be assessed analogously, by setting a fixed value of the parameter B. In this regard, Fig. 10 shows the sigmoids associated with values of a equal to 1.00, 0.50 and 0.25 with $B = 0.5$. Indeed, from the figure it can be observed that the sigmoids have the same shape but are translated horizontally. Specifically, considering a logarithmic scale to the base 10, the translation between two successive sigmoids is equal to

$$\log(N_2) - \log(N_1) = \log\left(\frac{A_2}{A_1}\right) = \log\left(\frac{a_2}{a_1}\right) = \log 2 = 0.301 \tag{11}$$

Moreover it should be noted that, for a fixed B value, as the parameter a decreases, the sigmoids shift to the left, indicating that in these conditions the phenomenon of TDC (in terms of both initiation and propagation) occurs earlier.

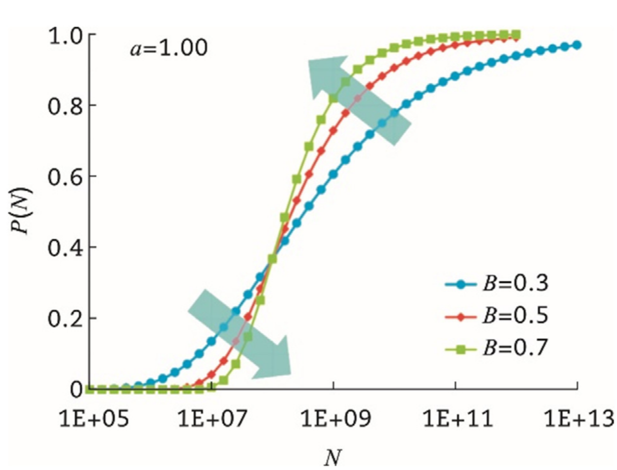

Fig. 9 – Influence of the shape parameter B on the normalized sigmoidal model P(N).

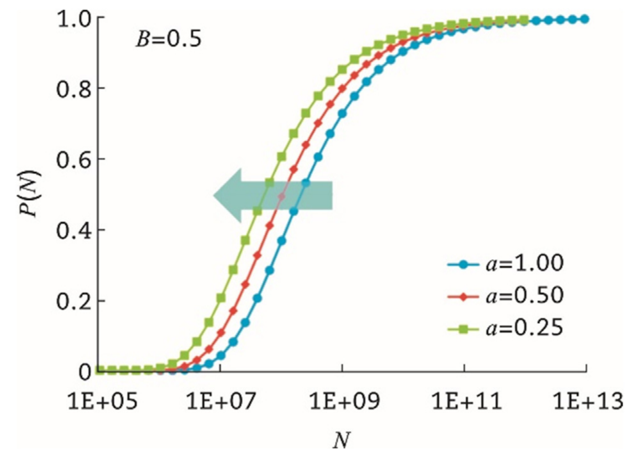

Fig. 10 – Influence of the translation factor A on the normalized sigmoidal model P(N).

3.3. *Application of the model to the experimental data*

In order to fit the model to the experimental data, Eq. (2) was rewritten as follows.

$$TDC(N) = TDC_{max}\, e^{-\left(\frac{A}{N}\right)^B} = TDC_{max}\, e^{-\left(\frac{a}{n}\right)^B} \tag{12}$$

where n is the number of 12-ton fatigue ESALs (N) scaled by a factor equal to 10^8, a and B are respectively the translation factor A scaled by a factor equal to 10^8 and the shape parameter. Analytical values for a and B were expressed in turn parametrically as functions of the OGFC mixture properties affecting the phenomenon. As can be seen from Eqs. (13) and (14), the shape parameter B was associated with the mechanical properties of the OGFC mixture, whereas the translation factor A was associated with the age of the OGFC mixture.

$$a = \frac{A}{10^8} = \alpha_1 - \alpha_2 \text{OGFC age} \tag{13}$$

$$B = \beta_1 - \beta_2 \text{ITS} \tag{14}$$

where α_1, α_2, β_1, β_2 are constants to be determined, OGFC age is the age of the OGFC mixture, ITS is the indirect tensile strength of the OGFC mixture.

As for the shape parameter, in Section 3.2 it was shown that higher values of B imply a delayed crack initiation but also an earlier achievement of the final stage of the distress. Therefore, such parameter was linked with the OGFC mixture properties, assessed through the ITS parameter (in turn, well correlated with the stiffness and the air void content of the mixture, as shown in Figs. 4(a) and 5). Once again, it should be noted that the use of the CT_{index} parameter for the evaluation of the mechanical properties of the mixture did not lead to meaningful results (Figs. 6 and 7), even though more experimental data are necessary to draw a firm conclusion on the applicability of CT_{index}.

At the same time, the decision to associate the translation factor a (or, analogously, A) with the OGFC age was due to the fact that the scientific literature documents a progressive worsening of the TDC resistance of the mixture as aging develops (Alae et al., 2021; Luo et al., 2018; Myers and Roque, 2002; Roque et al., 2010; Svasdisant et al., 2002). Therefore, for a fixed mixture, the shape of the sigmoid remains unchanged over time, but the effect of aging is taken into account through a progressive translation of the sigmoid to the left.

The proposed semi-empirical model (Eq. (12)) was applied to the experimental data summarized in Table 4. Specifically, the model parameters α_1, α_2, β_1, β_2 were determined by minimizing the error between model and experimental data, in order to achieve the best fitting. The results are shown in Fig. 11 ("model 1"), from which it is evident that the fitting is not good. In fact, the data are scattered and do not align along the bisector of the graph, and the parameters considered to assess the goodness of fit are not satisfactory (χ^2, which represents the error between model and experimental data, is too high and the determination coefficient R^2 is too low).

In order to provide a possible explanation, the measured TDC depths and the calculated TDC depths (model 1) were graphed as a function of OGFC age in Fig. 12. It can be seen that there seem to be some anomalies in the measured TDC depth values. These outliers, highlighted by boxes, may be due to the amount of RAP in the mixture (absent or excessive) or to the fact that some of the analyzed sections could be affected also by bottom-up cracking in advanced stage. In this second case, the top-down and bottom-up cracks could connect, leading to an erroneous assessment of TDC depth (even higher than TDC_{max}, assumed equal to 150 mm). Moreover, to explain the inaccuracy of the model, it should be considered also that the tested cores were taken from different motorway sections and that it was not possible to strictly comply with the testing protocols in all cases, as already explained in Section 2.3.

However, since the main purpose of this study was to develop a promising model to be adopted in the routine controls of a PMS, the possible outliers were excluded for the above-mentioned reasons and the model parameters were determined again ("model 2"). In this case, a very good fitting of the model to the experimental data was obtained, as demonstrated by the alignment of the data along the bisector of the graph and by a determination coefficient R^2 of 0.85 in Fig. 13.

Finally, the model parameters α_1, α_2, β_1, β_2 obtained (Fig. 13) were used to develop the sigmoids associated with the experimental data taken into consideration, as shown in Fig. 14. It is worth noting that, for all sampling points considered, the number of 12-ton fatigue ESALs was around 10^8 (Table 1). Therefore, data referring to different values of applied traffic loads should also be considered in the future.

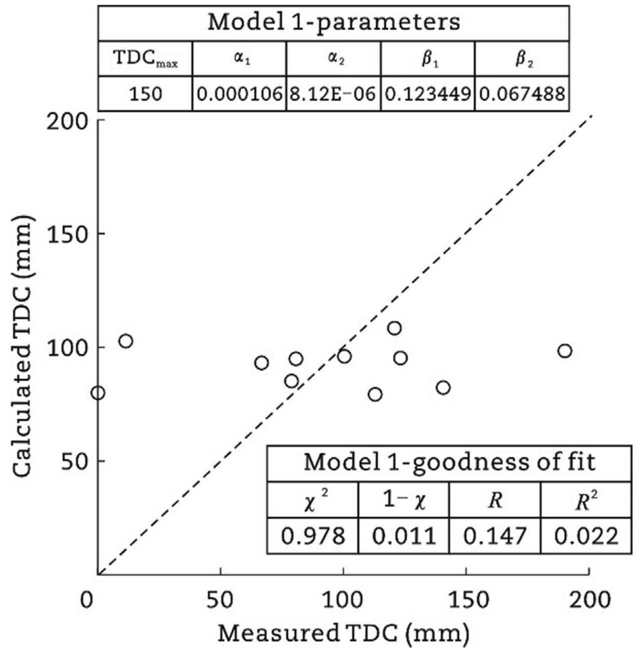

Fig. 11 – Comparison between measured TDC and calculated TDC (model 1).

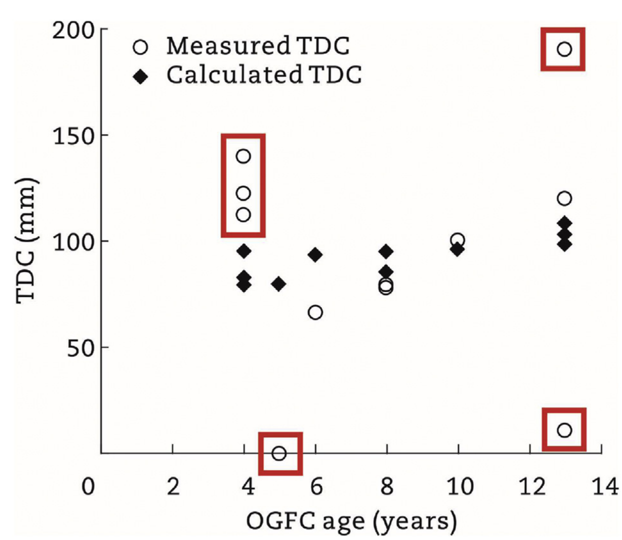

Fig. 12 – Comparison between measured TDC and calculated TDC (model 1) as a function of OGFC age.

Table 4 – Experimental data used for the model fitting.

Sampling point	OGFC age (years)	12-ton fatigue ESALs	Average TDC depth (mm)	ITS (MPa)
1	8	1.15E+08	80.0	0.69
2	10	8.70E+07	100.0	0.69
3	13	1.73E+08	11.0	0.88
4	5	7.72E+07	0.0	1.10
5	Intact core damaged during the coring operations (ITS not available)			
6	Intact core damaged during the coring operations (ITS not available)			
7	8	9.99E+07	78.5	1.00
8	13	1.70E+08	120.0	0.73
9	4	6.32E+07	140.0	0.99
10	4	6.32E+07	112.5	1.08
11	4	6.32E+07	122.5	0.54
12	13	1.73E+08	190.0	0.99
13	6	1.10E+08	66.5	0.71

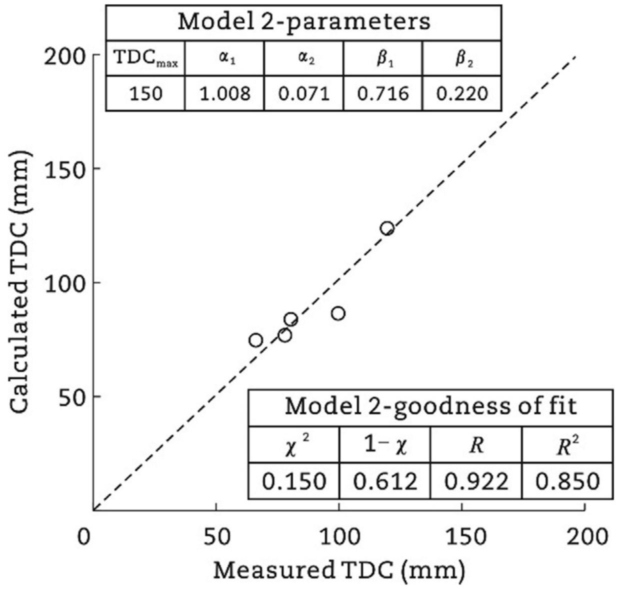

Fig. 13 – Comparison between measured TDC and calculated TDC (model 2).

3.4. *Considerations on the translation factor and the shape parameter*

Given the values of the model parameters α_1, α_2, β_1 and β_2 obtained (Fig. 13), the translation factor a and the shape parameter B can be written as follows.

$$a = \frac{A}{10^8} = 1.008 - 0.071\text{OGFC age} \quad (15)$$

$$B = 0.716 - 0.22\text{ITS} \quad (16)$$

From Eq. (15) it can be noted that, when the age of the asphalt mixture is zero (i.e., at the time of laying) the translation factor a is substantially equal to 1, and therefore the normalized N (normalized number of ESALs) is exactly equal to N (number of ESALs). In addition, as the mixture age increases, the value of the translation factor a becomes progressively smaller (lower than 1). As already discussed in Section 3.2, the reduction of a determines a translation of the sigmoid to the left, namely earlier initiation and propagation of the crack (Fig. 10). This finding supports the reliability of the proposed model, as it is well known that aging progressively reduces the resistance of the pavement to TDC (as already discussed in Sections 1 and 3.3). For simplicity and considering also the meaning of the condition $a = 1$, Eq. (15) could be rewritten as follows.

$$a = 1 - 0.07\text{OGFC age} \quad (17)$$

It is worth noting that, for an OGFC age of about 14 years, the parameter a (or A) is equal to zero, which means that TDC depth is equal to TDC_{max} (Eq. (12)). This is due to the fact that the oldest OGFC mixtures examined were 13 years old, as can be seen from Table 1. Therefore, to further improve the model prediction, older mixtures should be also considered. However, it should be pointed out that in most cases surface maintenance is carried out before the mixture reaches 13 years of in-service life (as demonstrated also by the data presented in Table 1).

Some interesting observations can be made also about the relationship between the shape parameter B and the mechanical properties of the OGFC mixture. Firstly, Eq. (16) suggests that the maximum value of B, associated with the minimum ITS value prescribed by the Italian technical specifications for open-graded mixtures ($\text{ITS}_{min} = 0.50$ MPa), is equal to $B_{max} = 0.61$. Moreover, as the ITS resistance of the

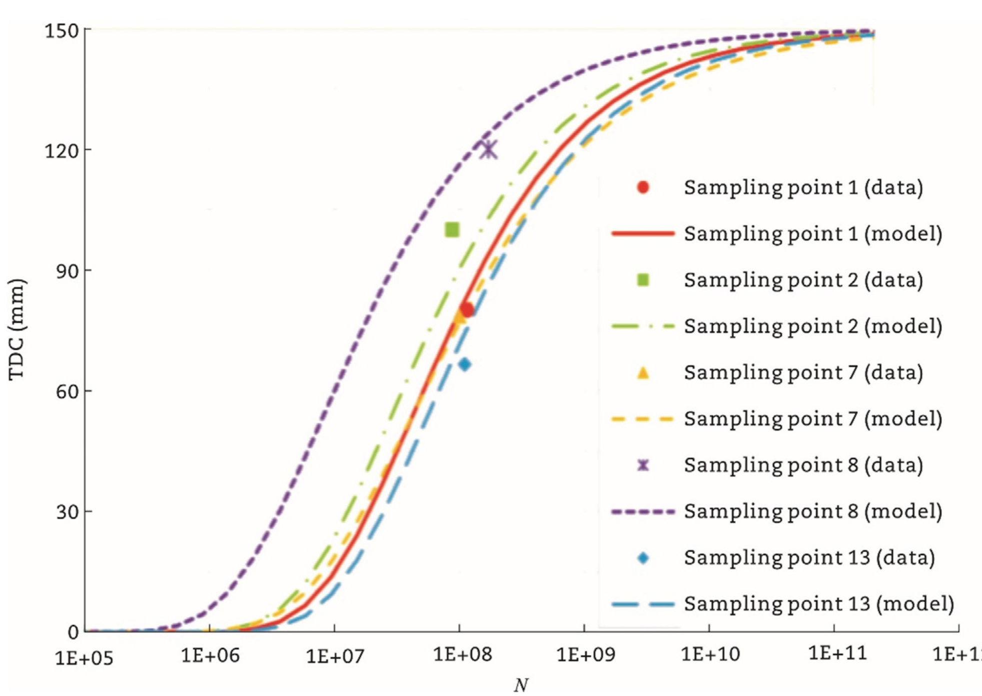

Fig. 14 – Sigmoids associated with the experimental data.

Fig. 15 – ARAN View image, September 2017.

mixture increases, the shape parameter B decreases, determining a progressive clockwise rotation of the sigmoid that corresponds to an earlier crack initiation (Fig. 9), as already discussed in section 3.2. This finding is in agreement with the basic principles of fracture mechanics, according to which stiffer mixtures are generally characterized by greater stress concentration at local defects/flaws that promotes the crack initiation, once again suggesting the reliability of the model. The slower propagation determined by the reduction of B (Fig. 9) is probably attributable to the balance between stiffness, strength and air void content of the OGFC mixture.

Finally, since the typical range of ITS values for open-graded mixtures is between 0.5 and 1.0 MPa (as confirmed by the experimental results reported in Table 3), the corresponding range of the shape parameter B would be between 0.61 and 0.50. Assuming that Eq. (16) is valid also in the case of polymer modified dense-graded mixtures, the range of the shape parameter B would be between 0.50 and 0.39, as the ITS values for these mixes are typically between 1.0 and 2.0 MPa. As can be seen from Fig. 9 (showing sigmoids with $a = 1$ and $B = 0.3$, 0.5 or 0.7), this would suggest that dense-graded mixtures are characterized by earlier TDC initiation as compared to open-graded mixtures. This result is in contrast with the experience and thus seems unrealistic. Therefore, the proposed model has to be considered valid only in the case of OGFC, whereas the balance between stiffness, strength and air void content may have a different effect in terms of TDC for dense-graded wearing layers.

3.5. *Preliminary validation of the model through in-situ observations*

In-situ observations allowed a qualitative preliminary validation of the proposed model. The images in Figs. 15–18 show the evolution over time of the same pavement stretch on the Italian motorway network. These images were taken by the Automatic Road Analyzer (ARAN) equipment during the monitoring of the pavement roughness. In the section examined, the OGFC was laid down in 2014.

From Fig. 15, it can be noted that in September 2017 no crack was visible on the pavement surface. Fig. 16, however, shows that in April 2018 TDC was already in an advanced stage in the foreground area of the pavement, as denoted by the presence of parallel sister cracks close to the right wheel path. Due to this cracking condition, a 6 cm thick dense-

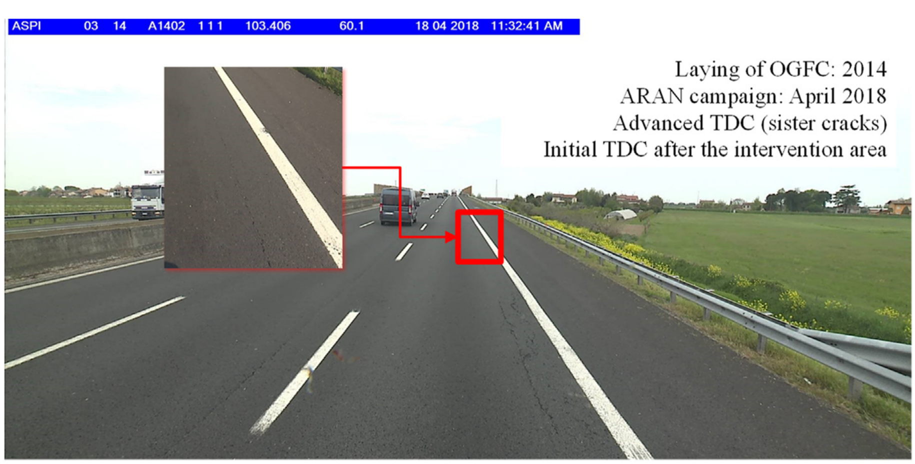

Fig. 16 – ARAN View image, April 2018.

Fig. 17 – ARAN View image, September 2018.

graded asphalt concrete (DGAC) patch was executed in July 2018, as can be observed from the images taken in September 2018 (Fig. 17).

In the pavement area immediately after the intervention area, from the zoom in Fig. 16 it is possible to observe the presence of TDC at the initial stage in April 2018. Finally, Fig. 18, dated back to May 2019, proves a worsening of TDC in the area after the patch, which is characterized by the presence of a clearly visible longitudinal crack.

In order to better investigate this cracking pattern, in May 2020 some cores were taken from the patch area and from the area affected by TDC, as shown in Fig. 19. From the extracted cores, no crack ascribable to TDC was found below the 6 cm thick patch, whereas a TDC depth of about 10 cm was observed in the area immediately after.

These in-situ observations (all summarized in Table 5) allow to state that in July 2018, at the time of the patching, TDC affected a thickness certainly lower than 6 cm, whereas in May 2020, in the area where no repair had been made, TDC had already reached a depth of 10 cm (note that in this area TDC was at the initial stage in April 2018 – Fig. 16). Therefore, a strong acceleration of TDC occurred in less than two years, consistently with the sudden and rapid growth of TDC depth predicted by the proposed sigmoidal model.

The previous considerations confirm the validity of the proposed model to predict the TDC distress and further underline the importance of timely identification of TDC, in order to implement immediate surface repairs that minimize the pavement damage and the maintenance costs.

4. Summary of the findings and future work

The main objective of this study was to develop a semi-empirical model for top-down cracking (TDC) depth evolution in thick asphalt pavements with open-graded friction course (OGFC). A series of cores were taken from different Italian motorway pavements affected by TDC and analyzed in the laboratory. Cracked cores taken from the wheel path were analyzed to determine TDC depth, whereas intact cores taken from the middle of the lane were tested to obtain the volumetric and mechanical properties of the OGFC mixture. The model was developed based on the results already available in literature, the outcomes of previous surveys on Italian motorway pavements and the findings of the laboratory investigation.

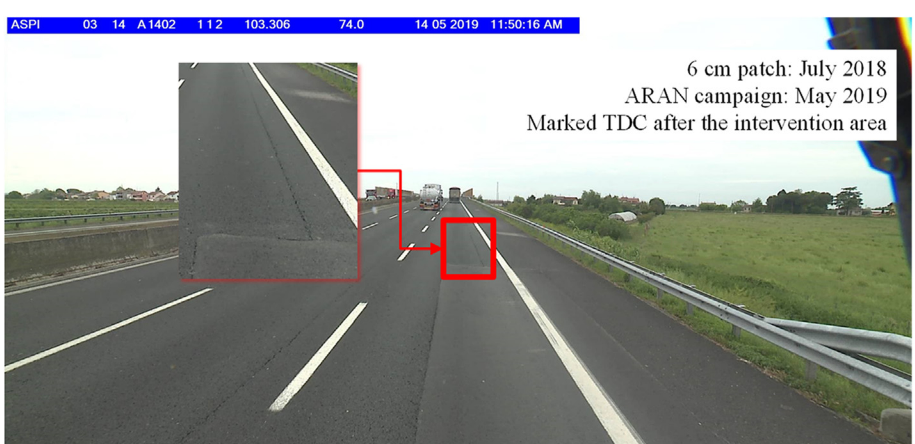

Fig. 18 – ARAN View image, May 2019.

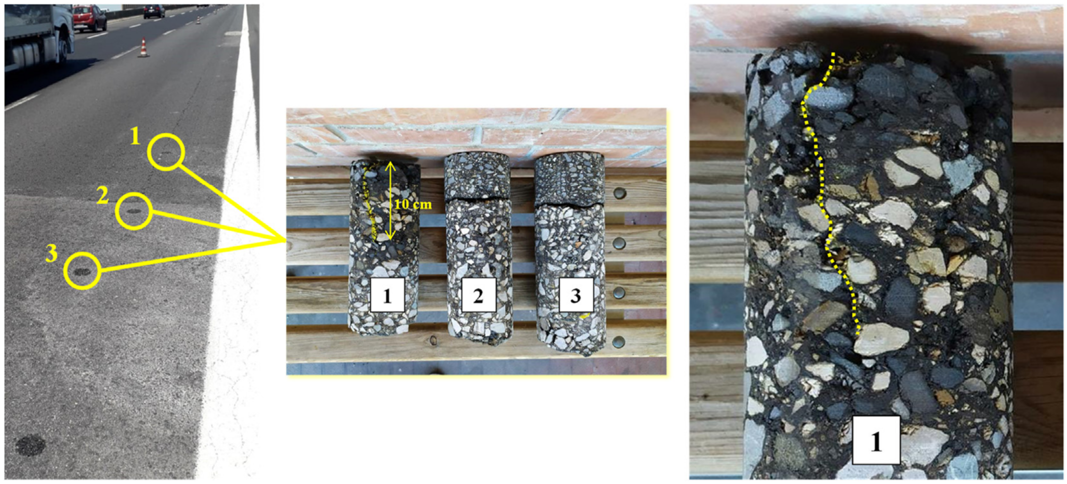

Fig. 19 – Cores taken from the pavement in May 2020.

Table 5 – Evolution of the monitored pavement stretch.

Date	Intervention area	After the intervention area
2014	Laying of OGFC	Laying of OGFC
September 2017	No crack	No crack
April 2018	Advanced TDC (sister cracks)	Initial TDC
July 2018	6 cm patch	No repair
September 2018	Patch in good conditions	Initial TDC
May 2019	Patch in good conditions	Marked TDC
May 2020	No TDC below the patch (coring)	TDC depth: 10 cm (coring)

The main findings of the study are the following.

- The crack depth observed on the cracked cores varied from 0 (TDC at early initiation stage) to 190 mm (possible influence of bottom-up cracking).
- The air void content measured on the intact cores varied between 14% and 28%. Older OGFCs were characterized by higher air voids, more recent OGFCs by lower air voids, consistent with the changes undergone by the Italian technical specifications over time.
- For the intact cores, the indirect tensile strength (ITS) values were well correlated with the air void content and the indirect tensile stiffness modulus (ITSM) values. Conversely, the CT_{index} parameter (proposed in literature to characterize the TDC performance of asphalt mixtures) did not show satisfactory correlations with the volumetric and mechanical properties of the OGFC.
- The proposed model predicts the evolution of TDC depth as a function of the applied traffic loadings (in terms of 12-ton fatigue equivalent single axle loads (ESALs)). Based on literature information and field observations, the model is sigmoidal with a maximum TDC depth assumed equal to 150 mm. The shape parameter and the translation factor of the sigmoidal function depend respectively on the ITS and on the age of the OGFC mixture.
- As the OGFC age increases, the sigmoid rigidly translates to lower values of ESALs, i.e., crack initiation and propagation occur earlier. The increase in the ITS of the OGFC mixture determines a rotation of the sigmoid that implies an earlier crack initiation. These effects are consistent with the experience and the results available in literature.
- Considering all the experimental data, the model fitting was not good. After excluding some outliers, the model was able to predict the measured TDC depth very well.
- In-situ observations on the evolution over time of the same pavement stretch indicated a sudden and rapid growth of TDC depth from less than 6 cm to 10 cm in less than two years, providing a qualitative preliminary validation of the sigmoidal model.

The proposed model can be used in a pavement management system (PMS) with the aim of planning surface maintenance due to TDC in a timely manner, thus minimizing pavement damage and maintenance costs.

The refining process of the proposed model through the collection of more experimental data could lead to a more precise prediction of TDC. Moreover, the applicability of the model to the case of pavements with different characteristics (e.g., thin asphalt pavements, dense-graded wearing layers) needs further studies.

Conflict of interest

The authors do not have any conflict of interest with other entities or researchers.

Acknowledgments

The activities presented in this paper were sponsored by Autostrade per l'Italia S.p.A. (Italy), which gave both financial and technical support within the framework of the Highway Pavement Evolutive Research (HiPER) project. The results and opinions presented are those of the authors.

REFERENCES

Alae, M., Zhao, Y., Leng, Z., 2021. Effects of ageing, temperature and frequency-dependent properties of asphalt concrete on top-down cracking. Road Materials and Pavement Design 22 (10), 2289–2309.

ARA Inc, 2004. Guide for Mechanistic-Empirical Design of New and Rehabilitated Pavement Structures. NCHRP Project 1-37. NCHRP, Washington DC.

Autostrade per l'Italia, 2018. Capitolato Speciale d'Appalto–Parte Seconda: Norme Tecniche di Appalto. ASPES, Colborddo.

Baladi, G.Y., Schorsh, M., Svasdisant, T., 2003. Determining the Causes of Top-Down Cracks in Bituminous Pavements. Michigan Department of Transportation, Lansing.

Canestrari, F., Ingrassia, L.P., 2020. A review of top-down cracking in asphalt pavements: causes, models, experimental tools and future challenges. Journal of Traffic and Transportation Engineering (English Edition) 7 (5), 541–572.

Chen, C., 2020. Validation of Laboratory Cracking Tests for Field Top-Down Cracking Performance (PhD thesis). Auburn University, Auburn.

Chen, Y., Tebaldi, G., Roque, R., et al., 2013. Development of a composite specimen interface cracking (CSIC) test for top-down cracking. Journal of Testing and Evaluation 41 (4), 625–634.

Chen, Y., Tebaldi, G., Roque, R., et al., 2012. Effects of interface condition characteristics on open-graded friction course top-down cracking performance. Road Materials and Pavement Design 13 (S1), 56–75.

COST 334, 2001. Effects of Wide Single Tyres and Dual Tyres. European Commission, Directorate General Transport, Brussels.

Dauzats, M., Rampal, A., 1987. Mechanism of surface cracking in wearing courses. In: The 6th International Conference on the Structural Design of Asphalt Pavements, Ann Arbor, 1987.

EN, 2020. Bituminous Mixtures-Test Methods-Part 6: Determination of Bulk Density of Bituminous Specimens. 12697-06. Europe Union, Brussels.

EN, 2017. Bituminous Mixtures-Test Methods-Part 23: Determination of the Indirect Tensile Strength of Bituminous Specimens. 12697–23. Europe Union, Brussels.

EN, 2018. Bituminous Mixtures-Test Methods-Part 26: Stiffness. 12697–26. Europe Union, Brussels.

Evensen, R., Senstad, P., 1992. Distress and Damage Factors for Flexible Pavements. Norwegian Road Research Laboratory, Oslo, 1992.

Foley, G.D., Sharp, K.G., 2001. Relative Effects of Wide Base Radial Tyres on Pavement Performance. ARR 351. Australian Road Research Board, Melbourne.

Gerritsen, A.H., van Gurp, C.A.P.M., van der Heide, J.P.J., et al., 1987. Prediction and prevention of surface cracking in asphaltic pavements. In: The 6th International Conference on the Structural Design of Asphalt Pavements, Ann Arbor, 1987.

Harmelink, D., Aschenbrener, T., 2003. Extent of Top-down Cracking in Colorado. Colorado Department of Transportation, Denver.

Hugo, F., Kennedy, T.W., 1985. Surface cracking of asphalt mixtures in Southern Africa. Journal of the Association of Asphalt Paving Technologists 54, 454–501.

Im, S., Zhou, F., 2017. New and simpler cracking test method for asphalt mix designs. Transportation Research Record 2631, 1–10.

Ingrassia, L.P., Spinelli, P., Paoloni, G., et al., 2020. Top-down cracking in Italian motorway pavements: a case study. Case Studies in Construction Materials 13, e00442.

Koh, C., 2009. Tensile Properties of Open Graded Friction Course (OFGC) Mixture to Evaluate Top-Down Cracking Performance (PhD thesis). University of Florida, Gainesville.

Kumara, M.W., Gunaratne, M., Lu, J.J., et al., 2004. Methodology for random surface-initiated crack growth prediction in asphalt pavements. Journal of Materials in Civil Engineering 16 (2), 175–185.

Ling, M., Luo, X., Chen, Y., et al., 2019. A calibrated mechanics-based model for top-down cracking of asphalt pavements. Construction and Building Materials 208, 102–112.

Luo, X., Gu, F., Ling, M., et al., 2018. Review of mechanistic-empirical modeling of top-down cracking in asphalt pavements. Construction and Building Materials 191, 1053–1070.

Lytton, R.L., Luo, X., Ling, M., et al., 2018. A Mechanistic Empirical Model for Top Down Cracking of Asphalt Pavements Layers. Project 01-52. NCHRP, Washington DC.

Ma, Z., Liu, L., Sun, L., 2018. Investigation of top-down cracking performance of in-situ asphalt mixtures based on accelerated pavement testing and laboratory tests. Construction and Building Materials 179, 277–284.

Matsuno, S., Nishizawa, T., 1992. Mechanism of longitudinal surface cracking in asphalt pavement. In: The 7th International Conference on the Structural Design of Asphalt Pavements, Nottingham, 1992.

Mun, S., Guddati, M.N., Kim, Y.R., 2004. Fatigue cracking mechanism in asphalt pavements with viscoelastic continuum damage finite element program. Transportation Research Record 1896, 96–106.

Myers, L.A., Roque, R., 2002. Top-down crack propagation in bituminous pavements and implications for pavement management. Journal of the Association of Asphalt Paving Technologists 71, 651–670.

Myers, L.A., Roque, R., Ruth, B.E., et al., 1999. Measurement of contact stresses for different truck tire types to evaluate their influence on near-surface cracking and rutting. Transportation Research Record 1655, 175–184.

Nikolaides, A., Manthos, E., 2019. Determination of asphalt layer thickness above which load-induced strains initiate top-down cracking and the effect of asphalt stiffness variation between wearing course and rest of asphalt layers. In: The 7th International Conference 'Bituminous Mixtures and Pavements' (7ICONFBMP), Thessaloniki, 2019.

Pellinen, T., Rowe, G., Biswas, K., 2004. Evaluation of Surface (Top Down) Longitudinal Wheel Path Cracking. Purdue University, West Lafayette.

Roque, R., Zou, J., Kim, Y.R., et al., 2010. Top-down Cracking of Hot-Mix Asphalt Layers: Models for Initiation and Propagation. Project 1-42A. NCHRP, Washington DC.

Roque, R., Birgisson, B., Drakos, C., et al., 2004. Development and field evaluation of energy based criteria for top-down cracking performance of hot mix asphalt. Journal of the Association of Asphalt Paving Technologists 73, 229–260.

Shen, S., Zhang, W., Shen, L., et al., 2016. A statistical based framework for predicting field cracking performance of asphalt pavements: application to top-down cracking prediction. Construction and Building Materials 116, 226–234.

Sun, L., Wang, G., Zhang, H., et al., 2018. Initiation and propagation of top-down cracking in asphalt pavement. Applied Sciences 8 (5), 774.

Svasdisant, T., Schorsch, M., Baladi, G.Y., et al., 2002. Mechanistic analysis of top-down cracks in asphalt pavements. Transportation Research Record 1809, 126–136.

Uhlmeyer, J.S., Willoughby, K., Pierce, L.M., et al., 2000. Top-down cracking in Washington State asphalt concrete wearing courses. Transportation Research Record 1730, 110–116.
Wambura, J.H.G., Maina, J., Smith, H.R., 1999. Kenya bituminous materials study. Transportation Research Record 1681, 129–137.
Wu, H., Yu, J., Song, W., et al., 2020. A critical state-of-the-art review of durability and functionality of open-graded friction course mixtures. Construction and Building Materials 237, 117759.
Zhou, F., Im, S., Sun, L., et al., 2017. Development of an IDEAL cracking test for asphalt mix design and QC/QA. Road Materials and Pavement Design 18 (S4), 405–427.
Zhou, F., Newcomb, D., Gurganus, C., et al., 2016. Experimental Design for Field Validation of Laboratory Tests to Assess Cracking Resistance of Asphalt Mixtures. Project 09-57. NCHRP, Washington DC.

Francesco Canestrari is a full professor of roads, railways and airports and chair of the master degree in civil engineering at Università Politecnica delle Marche (Italy). Professor Canestrari is involved as principal investigator in several international research projects. His specialty areas include testing specifications, interface shear characterization of asphalt layers, reinforced pavements, rheological and performance based characterization of sustainable and innovative pavement materials.

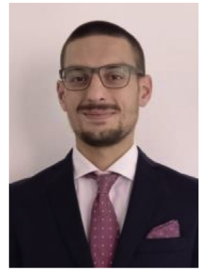

Lorenzo Paolo Ingrassia is a postdoctoral research fellow at Università Politecnica delle Marche (Italy). His areas of expertise include the rheological, chemical and performance-based characterization of sustainable and innovative pavement materials, the tribological characterization of asphalt binders, the investigation of reinforced pavements and the monitoring of in-service asphalt pavements.

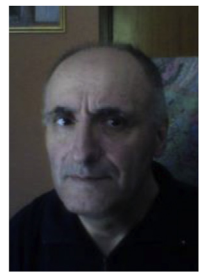

Amedeo Virgili is an associate professor of roads, railways and airports at Università Politecnica delle Marche (Italy). Professor Virgili specialty areas include road pavements and materials.